Fracture Mechanics of Concrete Structures
Proceedings FRAMCOS-3
AEDIFICATIO Publishers, D-79104 Freiburg, Germany

A Unified Modeling of Strain Localization in Concrete and its Finite Element Implementation

H.-W. Song, I.-S. Kim, U.-J. Na, and K.-J. Byun
Department of Civil Engineering, Yonsei University
Seoul, Korea

Abstract
Strain localization of concrete is a phenomenon such that the deformation of concrete is localized in finite region along with softening behavior. In this paper, a unified micromechanics-based model which can be applied to the analysis of the strain localization in concrete under both uniaxial tension and uniaxial compression is proposed and effective moduli are derived. Then, consistent algorithms for finite element modeling of the strain localization in concrete under compression are developed and applied to finite element analysis of the strain localization in concrete.
Key words : concrete, strain localization, unified model, consistent algorithm, finite element analysis

1 Introduction

Strain-localization behavior of quasi-brittle materials like concrete is a phenomenon such that the deformation of materials is localized in finite region along with post-peak strain-softening behavior. When the strain localization occurs in concrete, the deformation is

localized in finite zone and the final failure occurs in the localized zone. It is known that total behaviors or ultimate loads of concrete structures are governed by the localization behavior (Horii 1993). In this paper, a strain-localization model which is applicable for concrete member under both uniaxial compression and uniaxial tension is proposed by assuming that concrete under strain localization consists of localized zone and non-localized zone. From the proposed model, effective elastic moduli and modified effective elastic moduli of concrete under strain localization are obtained by applying micromechanical averaging techniques. For the finite element analysis of strain localization in concrete under compression, consistent algorithms are developed for the localized zone and non-localized zone by assuming that elasto-plastic strain-softening behavior occurs in the localized zone of concrete and damage unloading behavior occurs in the non-localized zone.

2 Unified model of strain-localization concrete

Fig. 1 shows strain-softening stress-strain curves obtained from compression test for different lengths of concrete specimens (van Mier 1986). Fig. 1 also shows that the size effect of post-peak behavior exists and the final failure is localized in finite region.

Based on the experimental observation, a concrete specimen under strain localization can be idealized with localized zone A and non-localized zone B as shown in Fig. 2(a). The stress-strain curves for two regions (curve A and curve B in Fig. 2(b)) can be obtained from measured deformations at each regions. After the peak, strain softening occurs in the localized zone and unloading occurs in the non-localized zone. The stress-strain curve of the specimen (i.e., curve C in Fig. 2(b)) is the averaged stress-strain curve.

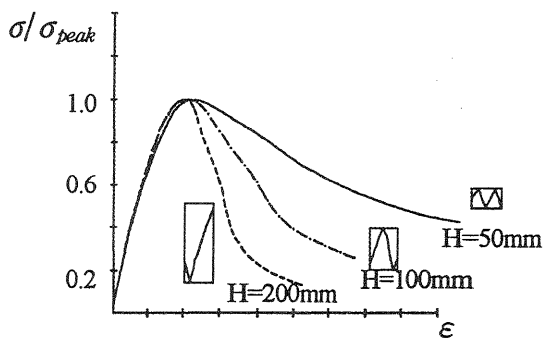

Fig. 1. Strain localization and size effect

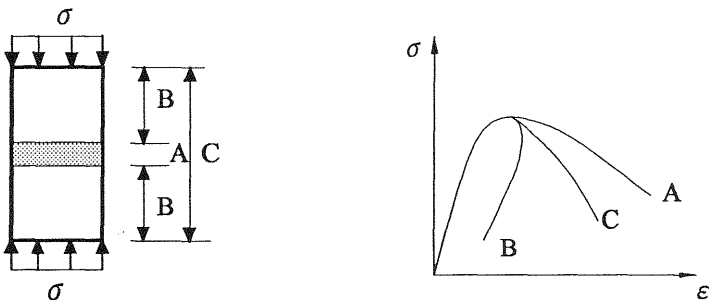

(a) specimen under uniaxial compression (b) stress-strain curves

Fig. 2. Model for strain localization of concrete

The finite localized zone can also be observed in tension test as in the compression test, but a major crack in the localized zone occurs and governs overall post-peak behavior of concrete.

In order to model the strain-localization phenomenon of concrete under both uniaxial compression and uniaxial tension in a unified manner, we consider that the strain localizes into finite size ΩL $(0 \leq \Omega \leq 1)$ in the concrete member of length L after the peak. The averaged strain increment $\langle \Delta\varepsilon \rangle_L$ after the peak of the specimen under strain localization can be written as,

$$\langle \Delta\varepsilon \rangle_L = \Omega \Delta\varepsilon_p + (1-\Omega)\Delta\varepsilon_u \tag{1}$$

where, $\Delta\varepsilon_p$ is strain increment in the localized zone, $\Delta\varepsilon_u$ is strain increment in the non-localized zone. Then, an effective elastic modulus E^* can be obtained from relationship between averaged stress increment $\langle \Delta\sigma \rangle_L$ and averaged strain increment $\langle \Delta\varepsilon \rangle_L$.

2.1 Effective moduli for uniaxial compression

Fig. 3 shows the concrete member under compression idealized as the softening behavior occurs $E_p < 0$ in the localized zone ΩL and the elastic unloading $E_u > 0$ in non-localized zone $(1-\Omega)L$. The averaged stress increment in the localized zone equals to that in the non-localized zone. Thus, an effective elastic modulus having size-effect parameter Ω can be obtained as follows,

$$E^* = \frac{E_p}{\Omega + (1-\Omega)\dfrac{E_p}{E_u}} \tag{2}$$

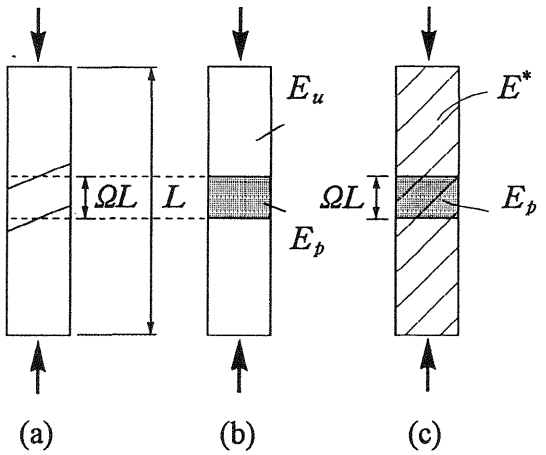

Fig. 3. Compression model for effective moduli

Using the self-consistent concept (Willis 1977), the E_u of the non-localized zone can be replaced by the E^* as shown in Fig. 3(c). Then, a modified effective elastic modulus can be derived as,

$$\overline{E^*} = \frac{E_p E_u}{\Omega E_u + (1-\Omega)[\Omega E_u + (1-\Omega) E_p]} \tag{3}$$

2.2 Effective moduli for uniaxial tension

The concrete member under the uniaxial tension is also assumed to have zone ΩL. But, in case of the uniaxial tension, a crack represented by crack opening displacement δ_f in the localized zone due to strain localization after the peak exists as shown in Fig 4(a). Using averaging technique, averaged strain increment $\langle \Delta\varepsilon \rangle_{\Omega L}$ in the localized zone ΩL after the peak stress can be written as,

$$\langle \Delta\varepsilon \rangle_{\Omega L} = \Delta\varepsilon_u + (\Omega L)^{-1} \Delta\delta_f \tag{4}$$

Then, an effective modulus $\overline{E_\Omega}$ for the localized zone ΩL can be obtained from the relationship between the averaged stress increment $\langle \Delta\sigma \rangle_{\Omega L}$ and the averaged strain increment $\langle \Delta\varepsilon \rangle_{\Omega L}$, i.e.,

$$\overline{E_\Omega} = \frac{D_f E_u}{D_f + (\Omega L)^{-1} E_u} \tag{5}$$

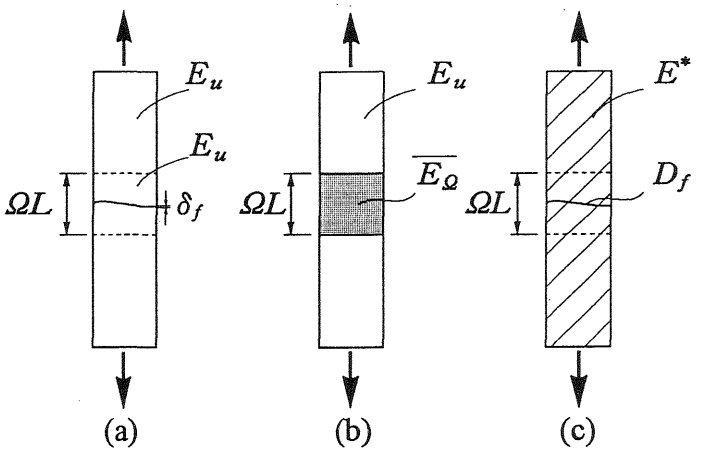

Fig. 4. Tension model for effective moduli

where D_f is the slope of tension-softening curve. By applying the averaging technique at the model of Fig. 4(b), one can obtain an effective modulus E^* as,

$$E^* = \frac{LD_fE_u}{D_fL + E_u} \tag{6}$$

Equation (6) shows that the modulus E^* includes the term L of size effect and is independent of the size of the localized zone ΩL. By the self-consistent concept, the E_u can be replaced by the E^* as shown in Fig. 4(c). Thus, a modified effective elastic modulus can be derived as follows.

$$\overline{E}^* = \frac{LD_fE_u}{2E_u + LD_f} \tag{7}$$

2.3 Analysis results and comparison with experiments

In order to verify the effective moduli derived from the proposed model, analysis results are compared with the experimental results by van Mier (1986) for uniaxial compression case and with those by Shah and Gopalaratnam (1985) for uniaxial tension case.

2.3.1 Uniaxial compression case

By using the effective moduli (eqns (2) and (3)) numerical analyses are performed for specimens having different lengths (50mm,

100mm, and 200mm). In the analysis, the post-peak softening curve by Saenz (1964) is used for E_p in the localized zone. The size of the localized zone ΩL is assumed to be N times of the maximum aggregate size $G_{\max}$ i.e., $\Omega L = NG_{\max}$. Figs. 5, 6, and 7 show the analysis results and comparisons with experimental results.

2.3.2 Uniaxial tension case

By using the effective elastic moduli (eqns (6) and (7)), numerical analyses are performed for different lengths of specimens (L, $2L$ and $4L$) under uniaxial tension. In the analysis, the D_f is obtained from the tension-softening curve proposed by Shah and Gopalaratnam (1985). Fig. 8 and Fig. 9 show analysis results and comparisons.

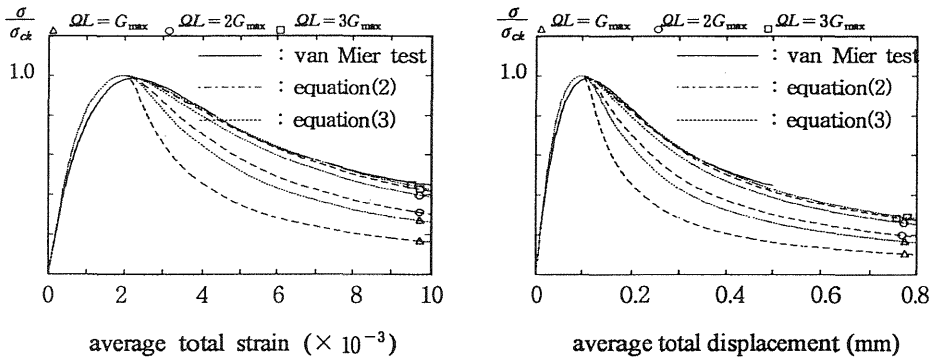

(a) stress-strain curves (b) stress-displacement curves

Fig. 5. L=50mm under uniaxial compression

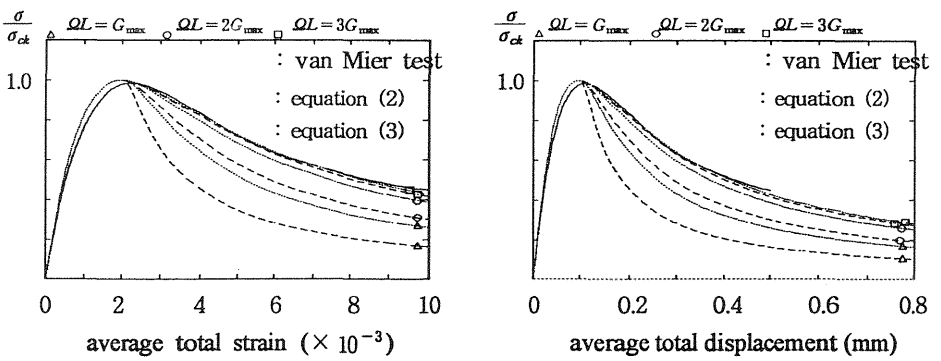

(a) stress-strain curves (b) stress-displacement curves

Fig. 6. L=100mm under uniaxial compression

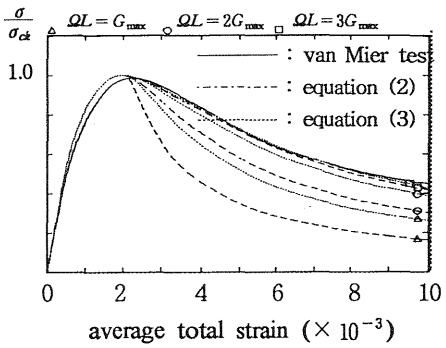

(a) stress-strain curves

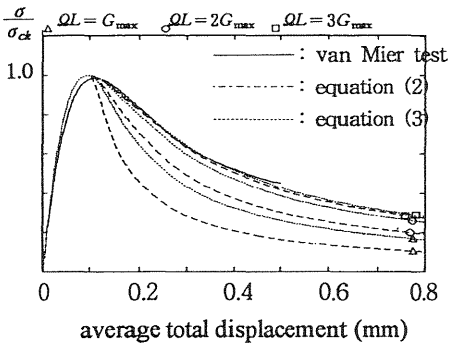

(b) stress-displacement curves

Fig. 7. L=200mm under uniaxial compression

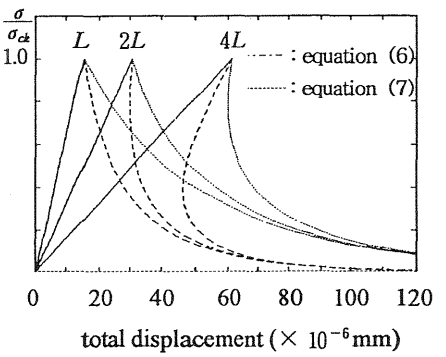

Fig. 8. Analysis results for uniaxial tension

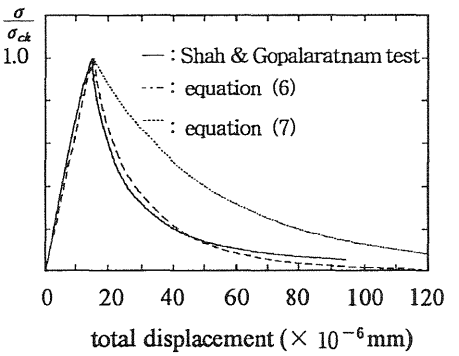

Fig. 9. Stress-displacement curves by uniaxial tension

3 Finite element modeling of strain localization under compression

3.1 Modeling of localized zone

For modeling of the localized zone in concrete under strain localization, a general Drucker-Prager failure criterion which can consider nonlinear strain softening as well as hydrostatic-pressure dependence of concrete is introduced in terms of the hydrostatic stress p, and effective plastic strain $\bar{e}^p$;

$$f(\boldsymbol{s}, p, \bar{e}^p) = \| \boldsymbol{s} \| - \sqrt{\frac{2}{3}} k(p, \bar{e}^p) = 0 \qquad (8)$$

where $\| \boldsymbol{s} \|$ is the norm of deviatoric stress $\boldsymbol{s}$. The $k(p, \bar{e}^p)$ in equation (8) can be written as follows.

$$k(p, \bar{e}^p) = k(\bar{e}^p) - \sqrt{\frac{3}{2}}\,\alpha \cdot p$$
$$= \sigma_0 + \bar{\sigma}\,\bar{e}^p + (\sigma_\infty - \sigma_0)[1 - e^{-\beta \bar{e}^p}] - \sqrt{\frac{3}{2}}\,\alpha \cdot p \tag{9}$$

where σ_0 is initial yield stress, $\bar{\sigma}$ is linear hardening modulus, σ_∞ is final yield stress, β is hardening exponent, and α is material parameter for hydrostatic-pressure dependence.

The return-mapping algorithm which is an effective procedure for integrating the elasto-plastic problem numerically is employed and a consistent tangent modulus (Simo and Taylor 1985) for the quadratic convergence of solution at iterations is derived as,

$$\mathbf{C}_{n+1} = K\mathbf{1}\otimes\mathbf{1} + 2G\bar{\beta}\left(\mathbf{I} - \frac{1}{3}\mathbf{1}\otimes\mathbf{1}\right) + \alpha K(\bar{r} - 1)\,\hat{\mathbf{n}}\otimes\mathbf{1} + 2G(\bar{r} - \bar{\beta})\,\hat{\mathbf{n}}\otimes\hat{\mathbf{n}} \tag{10}$$

where K is bulk modulus, G is shear modulus, $\hat{\mathbf{n}}\,(= \mathbf{s}/\|\mathbf{s}\|)$ is the unit vector normal to the yield surface, $\mathbf{1}$ is the second order unit tensor, and $\bar{\beta}$ and $\bar{r}$ are defined as follows, in which $k' = \dfrac{\partial k(\bar{e}^p)}{\partial \bar{e}^p}$ and $\mathbf{s}^T$ is elastic trial deviatoric stress.

$$\bar{\beta} = \frac{-\alpha p + \sqrt{\frac{2}{3}}k}{\|\mathbf{s}^T\|}, \quad \bar{r} = \frac{2}{3}\frac{k'}{2G + \frac{2}{3}k'} \tag{11}$$

3.2 Modeling of non-localized zone

During the strain localization of concrete, damage-unloading is assumed to occur in the non-localized zone. In order to consider nonlinear elastic-damage for the non-localized zone, the free energy function $\psi(\boldsymbol{\varepsilon}, q)$ is modified with $\bar{g}(q)$ as follows.

$$\psi(\boldsymbol{\varepsilon}, q) = \frac{1}{2}K(\mathbf{tr}\,\boldsymbol{\varepsilon})^2 + G\bar{g}(q)\,\|\mathbf{e}\|^2 \tag{12}$$

where $\mathbf{tr}\,\boldsymbol{\varepsilon}$ is trace of strain $\boldsymbol{\varepsilon}$, $\|\mathbf{e}\|$ is the norm of deviatoric strain $\mathbf{e}$, and $\bar{g}(q)$ is defined as,

$$\bar{g}(q) = \beta + (1-\beta)\frac{1 - e^{-q/\alpha}}{q/\alpha} \quad : \alpha \in [0,\infty],\ \beta \in [0,1] \tag{13}$$

where damage parameter $q = \| e \|$.

Using $\sigma = \frac{\partial \psi}{\partial \varepsilon}$, one can obtain a constitutive equation as,

$$\sigma = K(tr\,\varepsilon)1 + 2G\bar{g}(q)\,e \tag{14}$$

and the differentiation of equation (14) gives a consistent tangent modulus as follows.

$$C = K1 \otimes 1 + 2G[\,\bar{g}'(q) \cdot n \otimes e + \bar{g}(q) \cdot I_{dev}\,] \tag{15}$$

where $n = \frac{e}{\| e \|}$ and $I_{dev} = \frac{\partial e}{\partial \varepsilon}$.

3.3 Analysis results

For the finite element analysis of strain localization in concrete specimen under compression, three different lengths (L, $2L$ and $4L$) of concrete specimens having same size of localized zone $\Omega L\,(=0.4L)$ are analyzed and then three same size of specimens having different sizes ($0.1L$, $0.2L$ and $0.4L$) of the localized zone are also analyzed using finite element program implemented with the developed algorithms. The mesh size of an element in finite element discretization is constant as $0.1L$. In the analysis, the plastic material parameters adopted are $\sigma_0 = 0.243$, $\bar{\sigma} = -2$, $\sigma_\infty = 0.343$, $\beta = 10$ and $\alpha = 0.1$ and alos the damage material parameters $\alpha = 0.3$ and $\beta = 0.14$ are used. The analysis results as shown in Fig. 10 and Fig. 11, respectively, show that decrease in slopes of the stress-strain curve and stress-displacement curve in the post-peak

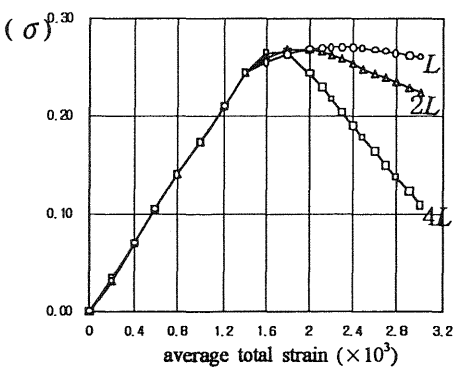

Fig. 10. Sress-strain curves for different specimen lengths

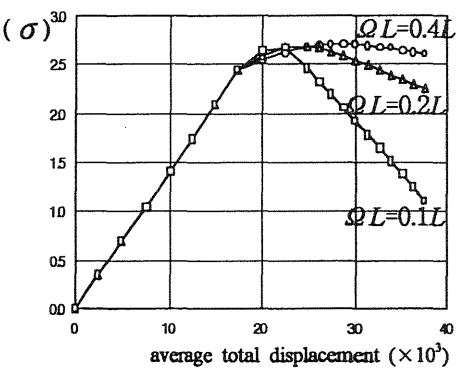

Fig. 11. Stress-displacement curves for different localized zone lengths

range, i.e., more softening behavior, is obtained by increasing specimen size or decreasing localized zone length as observed in the experiments (van Mier 1986).

4 Conclusion

In this paper, concrete under strain localization is modeled with localized zone and non-localized zone and the effective elastic moduli are derived by applying micromechanics-based averaging technique to the proposed model. Using the effective moduli, the concrete specimen under strain localization are analysed and compared with experimental results. Then, consistent algorithms for finite element analysis of strain localization behavior in concrete under compression are developed by considering plasticity and damage. Using finite element program implemented with the developed algorithms, strain-localization behaviors of concrete under compression are simulated.

References

Horii, H. (1993) Micromechanics and Localization in Concrete and Rock. in **Fracture and Damage of Concrete and Rock** (ed. H.P. Rossmanith), E.&F.N. Spon, London, 54-65.

Saenz, L. P. (1964) Discussion of Equation for the Stress-Strain Curve by Desai and Krishman. **ACI Journal**, Vol. 61, 1229-1235.

Shah, S. P., and Gopalaratnam, V. S. (1985) Softening Response of Plain Concrete in Direct Tension. **ACI Journal**, Vol. 82, 310-323.

Simo, J.C. and Taylor, R.L. (1985) Consistent Tangent Operators for Rate Independent Elastoplasticity. **Comp. Meth. Appl. Mech. Eng.**, 48, 101-108.

van Mier, J. G. M. (1986) Fracture of Concrete under Complex Stress. **Heron.** Heron Publication, Vol. 31, No. 3.

Willis, J. R. (1977) Bounds and Self Consistent Estimates for the Overall Properties of Anisotropic Composites. **J. Mech. Phy. Solids**, Vol. 25, 185-202.